Journal Pre-proofs

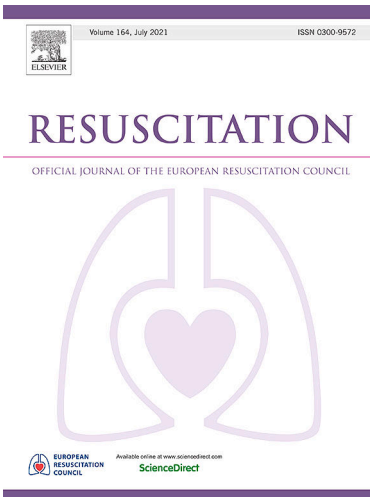

Clinical paper

CT Brain Perfusion Patterns and Clinical Outcome after Successful Cardiopulmonary Resuscitation: A Pilot Study

Arsany Hakim, Mattia Branca, Christoph Kurmann, Benedikt Wagner, Manuela Iten, Matthias Hänggi, Franca Wagner

PII: S0300-9572(24)00109-6
DOI: https://doi.org/10.1016/j.resuscitation.2024.110216
Reference: RESUS 110216

To appear in: *Resuscitation*

Received Date: 29 January 2024
Revised Date: 7 April 2024
Accepted Date: 8 April 2024

Please cite this article as: A. Hakim, M. Branca, C. Kurmann, B. Wagner, M. Iten, M. Hänggi, F. Wagner, CT Brain Perfusion Patterns and Clinical Outcome after Successful Cardiopulmonary Resuscitation: A Pilot Study, *Resuscitation* (2024), doi: https://doi.org/10.1016/j.resuscitation.2024.110216

CT Brain Perfusion Patterns and Clinical Outcome after Successful Cardiopulmonary Resuscitation: A Pilot Study

Arsany Hakim[1], Mattia Branca[2], Christoph Kurmann[1], Benedikt Wagner[1], Manuela Iten[3], Matthias Hänggi[3], Franca Wagner[1]

Affiliation:

1 University Institute of Diagnostic and Interventional Neuroradiology, Inselspital Bern University Hospital, and University of Bern, Bern, Switzerland

2 CTU Bern, University of Bern, Switzerland

3 Department of Intensive Care Medicine, Inselspital, Bern University Hospital, University of Bern, Bern, Switzerland

Corresponding author:

Arsany Hakim

arsany.hakim@insel.ch

University Institute of Diagnostic and Interventional Neuroradiology, Inselspital

Rosenbühlgasse 25,

3010 Bern

Switzerland

Word count:

Abstract: 269

Manuscript: 2982

Declaration of interest: none

Author contribution:

Arsany Hakim: Conceptualisation, methodology, formal analysis, data curation, visualisation, Writing– original draft

Mattia Branca: Formal analysis, writing– review and editing

Christoph Kurmann: Data curation, writing– review and editing

Benedikt Wagner: Data curation, writing– review and editing

Manuela Iten: Resources, data curation, writing– review and editing

Matthias Hänggi: Conceptualisation, resources, data curation, writing– review and editing

Franca Wagner: Validation, writing– review and editing

Graphical Abstract

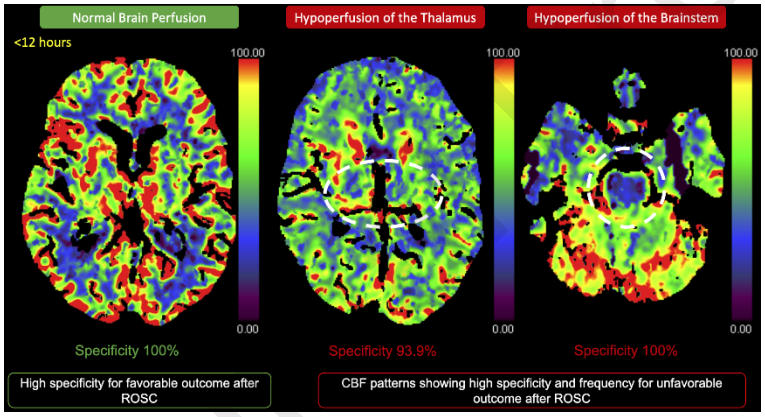

Highlights:

- 18 CT perfusion patterns were identified after post-cardiopulmonary resuscitation.
- Patterns such as brainstem hypoperfusion and coexisting hypoperfusion of the brainstem and thalamus are highly specific for unfavourable outcomes.
- Patterns may aid in stratifying patients and adjusting personalized treatment after resuscitation
- Normal perfusion within 12 hours after resuscitation predicts a favourable outcome with high specificity.

Abstract:

Aim:

CT perfusion is a valuable tool for evaluating cerebrovascular diseases, but its role in patients with hypoxic ischaemic encephalopathy is unclear. This study aimed to investigate 1) the patterns of cerebral perfusion changes that may occur early on after successful resuscitation, and 2) their correlation with clinical outcome to explore their value for predicting outcome.

Methods:

We conducted a retrospective analysis of perfusion maps from patients who underwent CT brain perfusion within 12 hours following successful resuscitation. We classified the perfusion changes into distinct patterns. According to the cerebral performance category (CPC) score clinical outcome was categorised as favourable (CPC 1–2), or unfavourable (CPC 3–5).

Results:

A total of 87 patients were included of whom 33 had a favourable outcome (60.6% male, mean age 60 ±16 years), whereas 54 exhibited an unfavourable outcome (59.3% male, mean age 60 ±19 years). Of the patients in the favourable outcome group, 30.3% showed no characteristic perfusion changes, in contrast to the unfavourable outcome group where all patients exhibit changes in perfusion. Eighteen perfusion patterns were identified. The most significant patterns for prediction of unfavourable outcome in terms of their high specificity and frequency were hypoperfusion of the brainstem as well as coexisting hypoperfusion of the brainstem and thalamus.

Conclusion:

This pilot study identified various perfusion patterns in patients after resuscitation, indicative of circulatory changes associated with post-cardiac-arrest brain injury. After validation, certain patterns could potentially be used in conjunction with other prognostic markers for stratifying patients and adjusting personalized treatment following cardiopulmonary resuscitation. Normal brain perfusion within 12 hours after resuscitation is predictive of favourable outcome with high specificity.

Keywords:

CT perfusion; brain; prognosis; hypoxic brain injury; cardiopulmonary resuscitation, post-cardiac-arrest brain injury

Abbreviations:

CBF: cerebral blood flow

CBV: cerebral blood volume

CPC: cerebral performance category

CPR: cardiopulmonary resuscitation

CTP: CT perfusion

FO: favourable outcome

MTT: mean transit time

NECT: non enhanced CT

NSE: Neuron specific enolase

PCABI: post-cardiac-arrest brain injury

ROSC: return of spontaneous circulation

Tmax: time to maximum of residue function

TTD: time to drain

TTP: time to peak

TTS: time to start

UO: unfavourable outcome

Introduction

Cardiac arrest is a significant global health issue with an incidence rate of 38–55 per 100,000 person-years [1]. Re-establishing the spontaneous circulation with restoration of the cerebral blood flow (CBF) to the ischaemic brain tissues can induce secondary brain injury and tissue inflammatory response, a condition known as post-cardiac-arrest brain injury (PCABI). PCABI causes changes in the cerebral perfusion [2], contributing significantly to mortality and morbidity following cardiac arrest.

Hypoxic brain injury remains the primary cause of death and long-term disability in patients who survive the acute phase after resuscitation [2], as 80% of patients after resuscitation are comatose due to PCABI and most of them die or suffer severe neurological disability [2]. Timely clinical evaluation of these patients is often challenging, due to the effects of therapeutic temperature management and sedatives. Multimodal outcome prognostication relies heavily on the absence of sedative medication. Hence, imaging markers play an important role in providing appropriate information to the relatives and in guiding treatment decision, particularly in severe cases of PCABI where recovery is unlikely.

CT perfusion (CTP) is a valuable tool in assessing changes of both the macro- and microvascular circulation. Yet, its role in the context of post-resuscitation care is underexplored. Our study aims to investigate perfusion patterns observed following cardiopulmonary resuscitation (CPR), aiming to improve our comprehension of imaging changes associated with cerebral perfusion after restoration of the circulation. Furthermore, we aim to explore the potential of these patterns as prognostic markers.

Methods

Patients and clinical data

The study was approved by the local ethics committee (KEK BE No. 126/15, KEK BE No. 2020-01761). We retrospectively analysed data from patients with cardiac arrest who were successfully resuscitated and subsequently underwent CTP, mainly for the detection or exclusion of ischemic lesions.

All patients who underwent scanning between 2014 and 2020 were considered for inclusion in the study, which was performed in accordance with the guidelines of the Declaration of Helsinki [3]. Written informed consent was obtained from all surviving patients or their next of kin. For patients who did not regain consciousness and subsequently died, their next of kin were informed and given the opportunity to object.

The primary inclusion criterion was availability of CTP acquired within 12 hours after resuscitation. Patients for whom clinical outcome data were unavailable were excluded.

Clinical data

Clinical data were retrospectively collected from our clinical information system and the Resuscitation Registry at Bern University Hospital by BW who was not involved in the rating. The results of the electroencephalogram (EEG) were classified into; benign, malignant and highly malignant patterns [4]. Additionally, neuron-specific enolase (NSE) levels were recorded, applying the threshold of 33ug/L to distinguish between favourable outcome (FO) and unfavourable outcomes (UO) [5]. Per guidelines, the decision regarding withdrawal of life-sustaining therapy was not made earlier than 96 h after ROSC [6].

Clinical outcomes were assessed according to the Glasgow-Pittsburgh Cerebral Performance Criteria (CPC) [7]. CPC 1 – as favourable clinical performance, CPC 2 – moderate cerebral disability, CPC 3 –severe cerebral disability, CPC 4 – coma and CPC 5 – death. For the purpose of our analysis, outcome was dichotomized into two categories, FO, which included CPC1 and 2, and UO, which included CPC 3, 4 and 5.

CT acquisition and postprocessing

The standard protocol at our institution includes a nonenhanced CT (NECT), CT angiography (CTA), followed by CTP. All scans were performed on a 128-multidetector CT (SOMATOM definition edge), and postprocessed using syngo.via VB10B (Siemens Healthcare, Erlangen, Germany). The methodology for CTP acquisition and postprocessing adheres to the procedure outlined in our previously published work [8].

Evaluation of images

The perfusion studies were evaluated by a board-certified neuroradiologist with over 15 years of imaging experience with a focus on diagnostic neurovascular and perfusion imaging. This evaluation aimed to identify and classify abnormal perfusion patterns. These were later verified by a second board-certified neuroradiologist with 15 years of experience. Both readers were blinded to patient outcomes. During the assessment, CTA was also reviewed to avoid pitfalls affecting perfusion interpretations, such as vascular stenosis, or vascular variants [9]. Additionally, NECT were evaluated by a single reader for signs indicative of hypoxia [10]. The findings were categorised as normal, equivocal or hypoxia.

Statistical analysis

Descriptive statistics are presented as frequencies and percentages for categorical variables and either mean with standard deviation (SD) or median with interquartile range (IQR) for continuous variables. Continuous variables were evaluated using Student's t-test or Wilcoxon-Mann-Whitney U-test, whereas categorical variables were evaluated using Fisher's exact test or the chi-squared test, as appropriate. For more than two groups, comparisons for continuous variables were made using either ANOVA or the Kruskal-Wallis test. Other measures of accuracy were computed, such as sensitivity, specificity, positive predicted value (PPV), negative predicted value (NPV) and accuracy with 95% confidence interval (CI). The statistical analysis was performed with the statistical software Stata 17.0 and R 4.3.1.

Results

Demographics

A search in PACS/RIS identified 846 patients with keywords 'Reanimation', 'REA' or 'ROSC'. Of these, only 109 patients underwent CTP. After excluding cases with missing outcomes, scanning >12 hours after resuscitation, unknown time to CT or suboptimal quality, the analysis included 87 patients, 33 patients in the favourable outcome (FO) group and 54 patients in the unfavourable outcome (UO) group (Fig. 1). The mean age was 60 (± 18) years, 52 male (59.8%).

No-flow, low-flow, and time to CT

Duration of no-flow phase was available for 80 patients. The median duration was recorded as zero minutes (indicating instances where it was less than a minute), with an IQR of 0-6 minutes. The duration of low-flow was available for 86 patients. The median duration was 21 minutes with an IQR of 10-35 minutes (Table 1).

Patterns

We identified 18 perfusion patterns: a) diffuse hypoperfusion of the supratentorial cortical grey matter, b) diffuse supra- and infratentorial hypoperfusion, c) regional cortical hypoperfusion, d) regional cortical hypoperfusion sparing the motor cortex, e) asymmetrical hypoperfusion, f) hyperperfusion – partial or global with perfusion delay, g) hypoperfusion of the basal ganglion, h) hypoperfusion of the globus pallidus (without involvement of other structures), i) hypoperfusion of the thalamus, j) hypoperfusion of the brainstem, k) cerebellar

hypoperfusion, l) supratentorial hypoperfusion with infratentorial hyperperfusion, m) hypoperfusion of the white matter, n) reduction in the gradient between grey and white matter in the colour coded CBV map, o) diffuse perfusion delay, p) bilateral border zone perfusion delay, q) regional perfusion delay, and r) territorial infarct(s). Fig. 2 provides a visual summary of these patterns. For comparison Fig 1 in the supplemental material shows a normal CT perfusion.

In this study, we observed 10 patients (11.5%) in the FO group had normal perfusion, while in the UO group, no patient exhibited normal perfusion. The diagnostic performance of normal perfusion for predicting FO was as follows: sensitivity 30%, specificity 100%, false negative rate 69.7%, false positive rate 0%, precision 100% and accuracy 74%. In the other patients, the patterns identified were observed either in isolation or in combination. Fig. 3 provides the frequencies of each perfusion pattern.

The sensitivity for prediction of UO was generally low whereas the specificity for several patterns was notably high. It exceeds 80% in: diffuse supra- and infratentorial hypoperfusion, regional cortical hypoperfusion, hypoperfusion of the basal ganglia, reduction in the gradient between grey and white matter in CBV, hyperperfusion and supratentorial hypoperfusion with infratentorial hyperperfusion (Table 2). Of particular significance were the perfusion patterns that demonstrated both high specificity (greater than 90%) and noteworthy frequency - “key patterns”: hypoperfusion of the thalamus, hypoperfusion of the brainstem, regional perfusion delay, and bilateral border-zone perfusion delay. Although certain patterns exhibited high specificity, their lower occurrence rate in our sample precluded them from being statistically significant indicators.

Concurrent patterns:

Coexistence of patterns was observed more frequently in the UO group. The most significant correlation occurred between diffuse hypoperfusion of the supratentorial gray matter and either diffuse perfusion delay or reduction in the gradient between gray and white matter. Additionally, a high correlation was found between hypoperfusion of the basal ganglia and either hypoperfusion of the thalamus, or reduction in the gradient between the gray and white matter (Fig 2 supplemental). However, after excluding patterns common to FO group, and less common patterns, concurrent hypoperfusion of thalamus and brainstem was frequently identified (n9) (Fig 4). This particular coexistence was not observed in the FO group. In the FO group, diffuse hypoperfusion of the supratentorial gray matter and diffuse perfusion delay commonly coexisting (n9); however, this coexistence was observed in 3 instances in the UO group (Fig 4) (Fig 3 supplemental).

NECT

Thirteen patients (24.1%) had signs of hypoxia, all of whom showed UO. In eight patients (9.2%) the signs were equivocal, six of them (11.1%) had UO. Sixty-six patients (75.9%) showed no signs of hypoxia and 35 out of those (64.8%) showed UO (Table 1 supplemental). In our cohort, the diagnostic performance of NECT for prediction of UO was as follows: sensitivity 24.1%, NPV 44.6%, specificity 100%, PPV 100%, and accuracy 52.9%.

Perfusion patterns and hypoxia signs on NECT

This subanalysis includes 74 patients who had either no signs of hypoxia or equivocal findings on NECT compared to 13 patients who showed clear signs of hypoxia. Different patterns were more prevalent in patients with hypoxic signs on NECT than in those without, specially hypoperfusion of the basal ganglia, hypoperfusion of the thalamus, diffuse perfusion delay and hyperperfusion.

Patterns that were more prevalent in patients without hypoxic signs on NECT include: diffuse hypoperfusion of the supratentorial cortical grey matter, regional perfusion delay, asymmetrical hypoperfusion, hypoperfusion of the white matter, and reduction in the gradient between grey and white matter in the CBV map (Fig. 4 supplemental)

Discussion:

In this study, we identified 18 patterns of perfusion changes occurring either in isolation or in combination following the restoration of circulation. These diverse perfusion patterns highlight the haemodynamic complexity inherent to the pathophysiology of hypoxia and help to improve our understanding of perfusion dynamics in this context. Although the sensitivity of these patterns in predicting UO was generally low, certain patterns had a particularly high specificity, such as hypoperfusion of the brainstem and thalamus. The high specificity of certain patterns suggests that they could be valuable in predicting UO, thereby aiding early decision-making and family counselling. It's noteworthy that a normal perfusion in the first 12 hours after ROSC predicts FO with very high specificity and precision.

Imaging plays a crucial role in management of patients after resuscitation, and extensive anoxic brain injury (seen in NECT or MRI) is one of the criteria used in the prognostication algorithm in the post resuscitation care as outlined in guidelines of the European Resuscitation Council and European Society of Intensive Care Medicine guidelines [11]. However, it is important to note that CT often yield false negative results. Despite its sensitivity, the use of MRI in the intensive care settings can be challenging. Risks associated with transporting critically ill patients and the complexity, or sometimes, unavailability of monitoring during MRI often limit its practicality.

CT scanners are widely available and are often utilised shortly after CPR. However, NECT typically fails to reveal the hypoxic changes early enough. In our sample, only 24.1% of patients exhibited signs of hypoxia on NECT in the UO group. CTA, while useful in assessing macrovascular pathologies, does not significantly contribute to the detection of hypoxic ischaemic injury, as these pathologies are not primarily related to macrovascular changes. In contrast, CTP emerges as a more helpful tool in this scenario. It provides information about intracranial vascular alterations, encompassing both the macrovascular and microvascular circulations. This capability makes CTP particularly valuable in assessing the complex vascular dynamics related to hypoxic brain injury.

Studies have highlighted that cerebral perfusion undergoes distinct phases following resuscitation[12] [13], illustrating the dynamic nature of perfusion changes and the critical importance of timing in perfusion imaging. PCABI features a series of circulatory changes resulting from global ischaemia and subsequent reperfusion which is often inhomogeneous and incomplete, leading to multifocal perfusion defects. The dynamics of CBF post-resuscitation follow a pattern of transient global hyperaemia, succeeded by a phase of delayed hypoperfusion, with a decrease in the metabolic rate and the oxygen extraction fraction. Further complexities arise from alterations in cerebral autoregulation, which can be disturbed, totally absent, or right shifted [14] [15] . In animal models, an increase in reduced CBF is not observed after increasing cerebral perfusion pressure due to a right shift [16]. Impaired autoregulation in the first 24 hours after resuscitation is associated with an UO, suggesting that autoregulation disturbances may contribute to additional brain damage [14]. Additionally, hypotension, which is common post-resuscitation, can negatively impact cerebral perfusion and exacerbate brain injury. It may be observed 15-60 minutes after ROSC, but can persist for hours or even days [12]. Furthermore, incomplete filling of the cortical capillary bed (the no-reflow phenomenon) can occur due to microcirculatory disturbances and perfusion deficit. This phenomenon may be associated with post-resuscitation hypotension, increased blood viscosity, and fibrin clots [12]. Another significant factor is the development of both cytotoxic and vasogenic oedema, which can lead to increased intracranial pressure [2]. The areas most commonly affected by the multifocal defects include the striatum, thalamus, and temporomesial structures [2] [17] [18]with grey matter being particularly vulnerable due to its high oxygen demand.

The variations in cerebral perfusion observed in our series can be largely attributed to the pathophysiological mechanisms underlying hypoxic brain injury. The diverse regional changes can be explained by the inhomogeneity of global ischaemia. The occurrence of hyperperfusion patterns could be linked to hyperaemia. Differences in the status of cerebral autoregulation could explain the variability among patients showing partly hypoperfusion and partly normal or hyperperfusion. Border-zone perfusion delays could be associated with hypotension. The presence of supratentorial hypoperfusion and infratentorial hyperperfusion suggests preferential perfusion to the posterior circulation[19]. Perfusion changes were more pronounced in grey matter. Significantly, in our cohort, certain patterns like hypoperfusion of the basal ganglia, thalamus and brainstem exhibited high specificity for UO. However, caution is required when evaluating CTP due to potential artefacts, particularly in regions such as the brainstem, as well as various technical factors that may lead to misinterpretation.

Consequently, expertise in CTP imaging analysis is crucial for accurate interpretation. The changes in perfusion imaging following resuscitation, and their subsequent recovery, may provide an opportunity to identify specific patterns that facilitate personalized medicine in PCABI for a case-based selection of the most effective treatment strategies and interventions.

Self-fulfilling prophecy represents a significant bias in prognostication [11], highlighting the importance of vigilance to mitigate its impact during evaluation. Relying solely on perfusion is inadequate. Since no single predictor is reliable serves as a prognostic marker, accurate prognostication after ROSC should ideally depend on a combination of clinical and paraclinical predictors. It is imperative for the treating team to integrate imaging with other clinical markers and to interpret them in the clinical context to ensure a comprehensive evaluation. Employing decision trees or a scoring system that combines various prognostic tests with different weights can minimise the risk of false predictions and enhances the reliability of assessment [2].

An ideal prognostic marker in this setting should have high specificity to ensure that no patient is mistakenly predicted to have UO. In our series, various perfusion patterns demonstrated high specificity, suggesting their potential utility as supplementary prognostic imaging markers. However, the precision of these patterns, as well as that of NECT, was relatively low. Therefore, our findings advocate for a balanced and comprehensive approach to prognostication, combining imaging findings with clinical assessment for more reliable prediction. Furthermore, CTP when revealing patterns suggestive of impaired autoregulation, can also guide therapy. For instance, it may inform targeted interventions for maintaining reasonable mean arterial pressure, hypertension, hemodilution, or thrombolytic therapy in patients who may benefit. However, for such targeted therapies, further studies incorporating quantitative analysis of CBF and simultaneous measurement of mean arterial pressure and brain oxygen levels could prove valuable [12] [15] [14] .

It is important to emphasise that the objective of our study was not to diagnose brain death, which involves confirming the absence of intracranial blood flow. Therefore, the results and conclusion drawn from our study should be interpreted within the specific context of hypoxic ischaemic injury.

Strengths

This study compared various perfusion patterns and their performance within the same patient cohort, including both FO and UO. The balanced groups facilitated a comparative analysis of the perfusion patterns' performance.

Limitations

This is a retrospective study, subject to selection bias, and included only patients who underwent a CTP within 12 hours from resuscitation. The small sample size limits the

generalizability of the findings and is also not statistically designed to internally validate a specific perfusion pattern.

The mesiotemporal structures were not specifically evaluated due to the limitations of CTP, which can produce artefacts in this region. The timing of imaging, the duration of no-flow, and low-flow varied among patients, introducing another layer of variation to the results. In most patients in our cohort CTP was performed only once, and only few cases examined after 12 hours, preventing us from tracking the evolution of this dynamic process in each individual patient across different post-resuscitation phases. Consequently, transient changes in perfusion could not be detected and the main outcome analysis focused on patients who underwent CTP within 12 hours post-resuscitation, mainly capturing the hypoperfusion phase. In some instances, the classification of UO may have influenced the decision to withdraw life support based on prognostic expectations, rather than actual death. Lastly, in this pilot study, we didn't perform correlations between the perfusion patterns, and other parameters such as the clinical status during the perfusion imaging, the sedation status or the mean arterial pressure.

Conclusion

This pilot study identified several perfusion patterns after cardiac arrest, that may have prognostic and pathophysiological significance in PCABI. Certain perfusion patterns demonstrated high specificity for UO. Further studies are needed to validate our findings and confirm patterns that could be used as additional markers for prognostic assessment.

Conflict of interest: none

This research did not receive any specific grant from funding agencies in the public, commercial, or not-for-profit sectors.

References:

[1] Gräsner J-T, Lefering R, Koster RW, Masterson S, Böttiger BW, Herlitz J, et al. EuReCa ONE□27 Nations, ONE Europe, ONE Registry. Resuscitation 2016;105:188–95. https://doi.org/10.1016/j.resuscitation.2016.06.004.

[2] Sandroni C, Cronberg T, Sekhon M. Brain injury after cardiac arrest: pathophysiology, treatment, and prognosis. Intensive Care Med 2021;47:1393–414. https://doi.org/10.1007/s00134-021-06548-2.

[3] World Medical Association Declaration of Helsinki. JAMA 2013;310:2191. https://doi.org/10.1001/jama.2013.281053.

[4] Westhall E, Rossetti AO, van Rootselaar A-F, Wesenberg Kjaer T, Horn J, Ullén S, et al. Standardized EEG interpretation accurately predicts prognosis after cardiac arrest. Neurology 2016;86:1482–90. https://doi.org/10.1212/WNL.0000000000002462.

[5] Zandbergen EGJ, Hijdra A, Koelman JHTM, Hart AAM, Vos PE, Verbeek MM, et al. Prediction of poor outcome within the first 3 days of postanoxic coma. Neurology 2006;66:62–8. https://doi.org/10.1212/01.wnl.0000191308.22233.88.

[6] Sandroni C, Cariou A, Cavallaro F, Cronberg T, Friberg H, Hoedemaekers C, et al. Prognostication in comatose survivors of cardiac arrest: An advisory statement from the European Resuscitation Council and the European Society of Intensive Care Medicine. Resuscitation 2014;85:1779–89. https://doi.org/10.1016/j.resuscitation.2014.08.011.

[7] Cummins RO, Chamberlain DA, Abramson NS, Allen M, Baskett PJ, Becker L, et al. Recommended guidelines for uniform reporting of data from out-of-hospital cardiac arrest: the Utstein Style. A statement for health professionals from a task force of the American Heart Association, the European Resuscitation Council, the Heart and Stroke Foundation of Canada, and the Australian Resuscitation Council. Circulation 1991;84:960–75. https://doi.org/10.1161/01.cir.84.2.960.

[8] Hakim A, Pastore-Wapp M, Vulcu S, Dobrocky T, Z'Graggen WJ, Wagner F. Efficiency of Iterative Metal Artifact Reduction Algorithm (iMAR) Applied to Brain Volume Perfusion CT in the Follow-up of Patients after Coiling or Clipping of Ruptured Brain Aneurysms. Sci Rep 2019;9:19423. https://doi.org/10.1038/s41598-019-55792-6.

[9] Hakim A, Gralla J, Rozeik C, Mordasini P, Leidolt L, Piechowiak E, et al. Anomalies and Normal Variants of the Cerebral Arterial Supply: A Comprehensive Pictorial Review with a Proposed Workflow for Classification and Significance. Journal of Neuroimaging 2017. https://doi.org/10.1111/jon.12475.

[10] Huang BY, Castillo M. Hypoxic-Ischemic brain injury: Imaging findings from birth to adulthood. Radiographics 2008. https://doi.org/10.1148/rg.282075066.

[11] Nolan JP, Sandroni C, Böttiger BW, Cariou A, Cronberg T, Friberg H, et al. European Resuscitation Council and European Society of Intensive Care Medicine guidelines

2021: post-resuscitation care. Intensive Care Med 2021;47:369–421. https://doi.org/10.1007/s00134-021-06368-4.

[12] Iordanova B, Li L, Clark RSB, Manole MD. Alterations in cerebral blood flow after resuscitation from cardiac arrest. Front Pediatr 2017. https://doi.org/10.3389/fped.2017.00174.

[13] van den Brule JMD, van der Hoeven JG, Hoedemaekers CWE. Cerebral Perfusion and Cerebral Autoregulation after Cardiac Arrest. Biomed Res Int 2018;2018:1–5. https://doi.org/10.1155/2018/4143636.

[14] Ameloot K, Genbrugge C, Meex I, Jans F, Boer W, Vander Laenen M, et al. An observational near-infrared spectroscopy study on cerebral autoregulation in post-cardiac arrest patients: Time to drop 'one-size-fits-all' hemodynamic targets? Resuscitation 2015;90:121–6. https://doi.org/10.1016/j.resuscitation.2015.03.001.

[15] Sundgreen C, Larsen FS, Herzog TM, Knudsen GM, Boesgaard S, Aldershvile J. Autoregulation of Cerebral Blood Flow in Patients Resuscitated From Cardiac Arrest. Stroke 2001;32:128–32. https://doi.org/10.1161/01.STR.32.1.128.

[16] Christopherson TJ, Milde JH, Michenfelder JD. Cerebral Vascular Autoregulation and CO_2 Reactivity following Onset of the Delayed Postischemic Hypoperfusion State in Dogs. Journal of Cerebral Blood Flow & Metabolism 1993;13:260–8. https://doi.org/10.1038/jcbfm.1993.32.

[17] Barth R, Zubler F, Weck A, Haenggi M, Schindler K, Wiest R, et al. Topography of MR lesions correlates with standardized EEG pattern in early comatose survivors after cardiac arrest. Resuscitation 2020;149:217–24. https://doi.org/10.1016/j.resuscitation.2020.01.014.

[18] Wagner F, Hänggi M, Weck A, Pastore-Wapp M, Wiest R, Kiefer C. Outcome prediction with resting-state functional connectivity after cardiac arrest. Sci Rep 2020;10:11695. https://doi.org/10.1038/s41598-020-68683-y.

[19] Hakim A, Wagner F. Preferential Perfusion to the Posterior Circulation in Hypoxia. Ann Neurol 2023;93:417–8. https://doi.org/10.1002/ana.26539.

Legends to figures

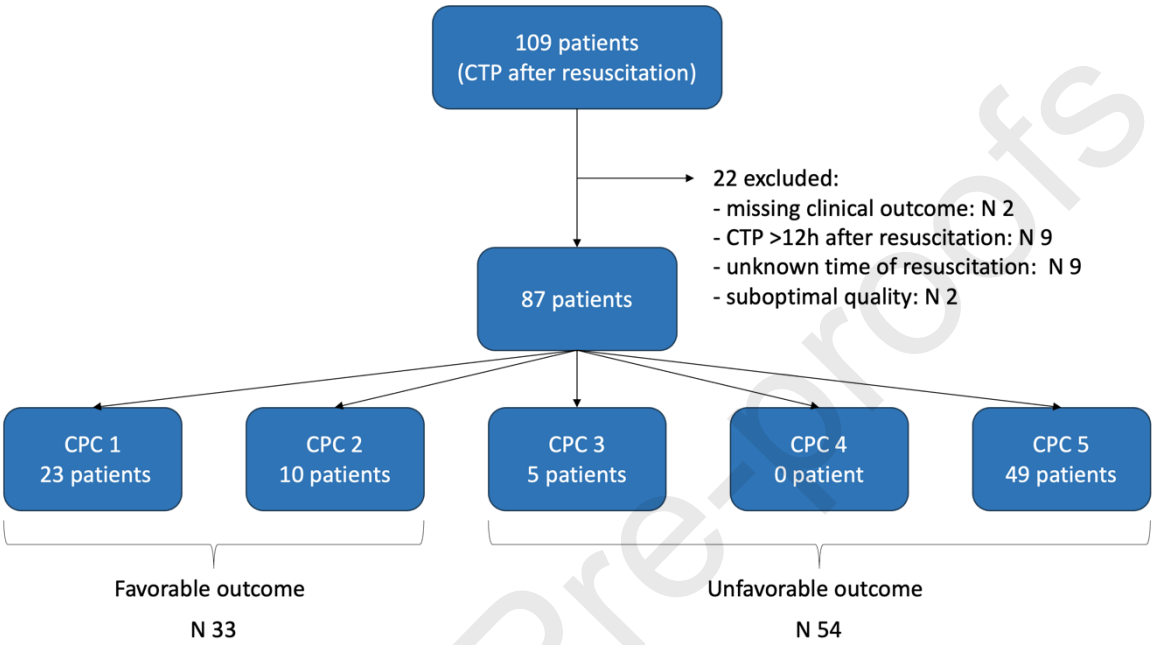

Fig. 1: Flow diagram showing the process for inclusion and exclusion in the study population.

Abbreviations: CPC = cerebral performance category, CTP = CT perfusion.

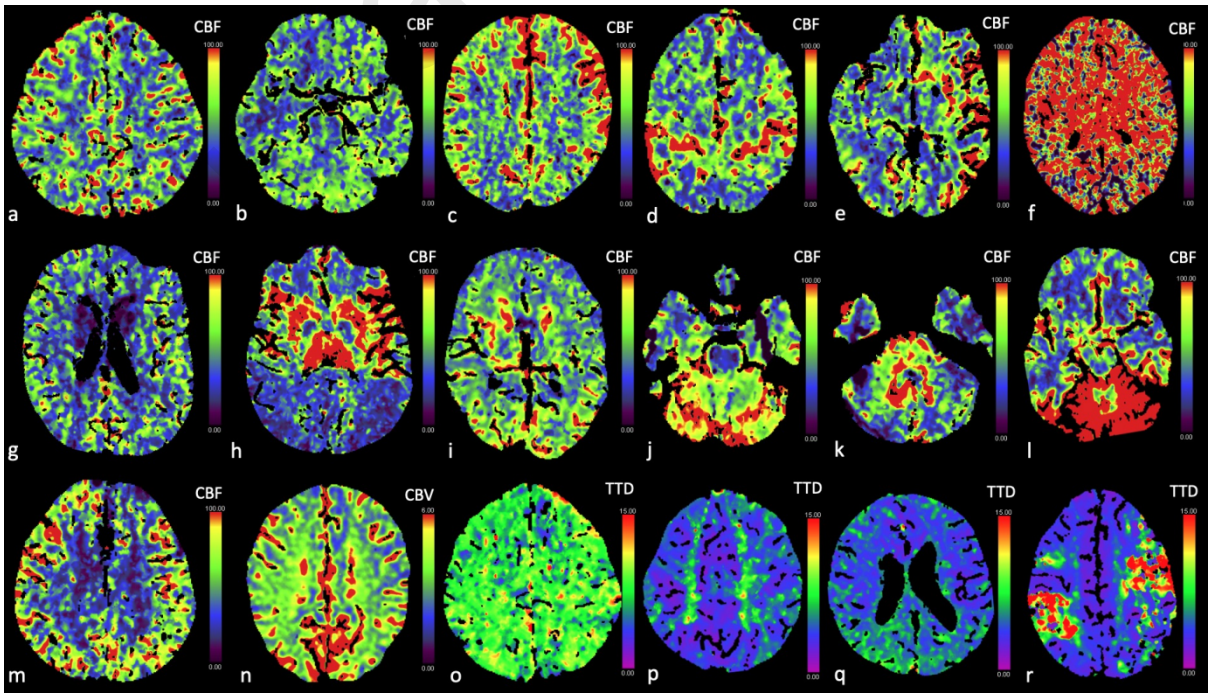

Fig. 2: Visual summary of the 18 perfusion patterns identified in the study, taken from 16 different patients. Cerebral blood flow (CBF) (a–m), cerebral blood volume (CBV) (n) and time to drain (TTD) (o–r) parametric maps: a) diffuse hypoperfusion of the supratentorial cortical grey matter, b) diffuse supra- and infratentorial hypoperfusion, c) regional cortical hypoperfusion, d) regional cortical hypoperfusion sparing the motor cortex, e) asymmetrical hypoperfusion, f) hyperperfusion, g) hypoperfusion of the basal ganglia, h) hypoperfusion of the globus pallidus, sparing other basal ganglia, i) hypoperfusion of the thalamus, j) hypoperfusion of the brainstem, k) hypoperfusion of the cerebellum, l) supratentorial hypoperfusion with infratentorial hyperperfusion, m) hypoperfusion of the white matter, n) reduction in the gradient between grey and white matter on CBV, o) diffuse perfusion delay, p) bilateral border zone perfusion delay, q) regional perfusion delay, r) territorial infarct(s). Subfigure a and o as well as subfigures l and p are from the same patients, otherwise the subfigures are taken from different patients.

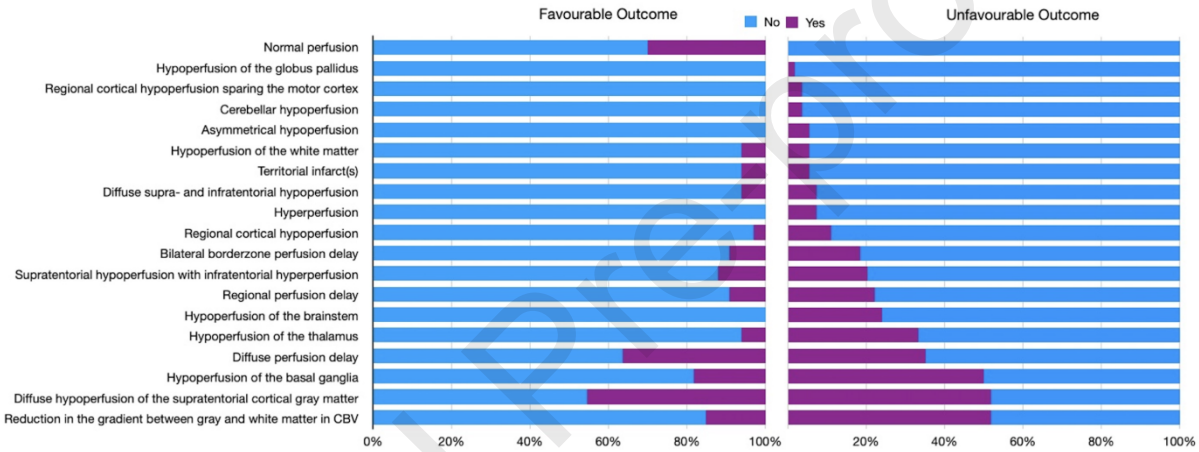

Fig. 3: Stacked column chart illustrates the frequency of each perfusion pattern identified in both the favourable and unfavourable outcome groups.

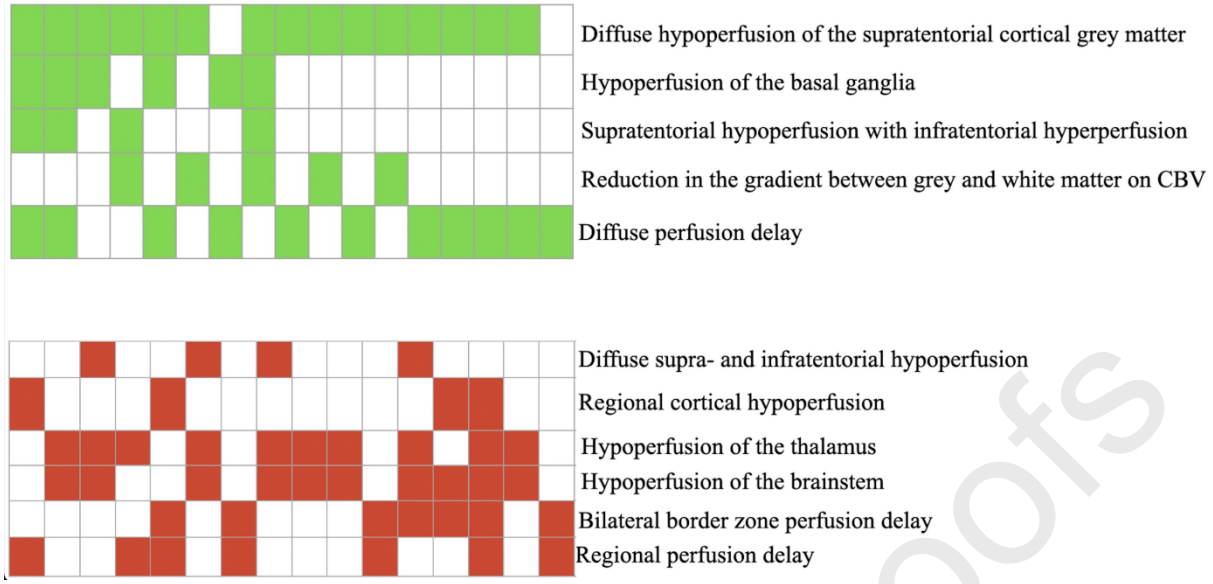

Fig. 4: Binary matrix illustrating the coexisting patterns in the favourable outcome group (green) and unfavorable outcome group (red). For simplification, patients without patterns and those with infrequent patterns (fewer than 4 occurances) were excluded. Additionally, patterns frequently found in the favourable outcome group were removed from the binary matrix representing the unfavourable outcome group. It is demonastrated that coexisting hypoperfusion of the brainstem and thalamus is common in the unfavorable outcome group, while diffuse hypoperfusion of the supratentoiral gray matter accompanied by diffuse perfusion delay is commonly observed in the favourable outcome group.

Tables:

	Total	Favourable outcome	Unfavourable outcome	Mann-Whitney statistic, mean difference or risk difference (95% CI)	P value
Number	87	33 (37.9%)	54 (62%)		
Age					
Mean (SD) y	60 (18)	60 (16)	60 (19)	0.51 (-7.5 to 8.5)	0.90

Median [lq, uq]	62 [49,74]	62 [52,71]	65 [47,75]	0.49 (0.37 to 0.61)	0.83
Sex (M) - n (%)	52 (59.8%)	20 (60.6%)	32 (59.3%)	1.3% (-19.9 to 22.6%)	0.90
Duration of no-flow, min*					
mean (SD)	4.1 (6.2)	2.0 (5.8)	5.3 (6.2)	-3.3 (-6.1 to -0.55)	0.020
median [lq, uq]	0.00 [0.00,6.0]	0.00 [0.00,1.0]	5.0 [0.00,10]	0.31 (0.21 to 0.43)	0.002
Duration of low flow, min#					
Mean (SD)	24 (17)	17 (14)	29 (18)	-12 (-19 to -4.7)	0.001
Median [lq, uq]	21 [10,35]	11 [6.5,23]	26 [15,40]	0.28 (0.19 to 0.41)	<0.001
EEG classification according to Westhall n (%) †					<0.001
Normal	1 (2.9%)	0 (0.0%)	1 (4.2%)	-4.2% (-12.2 to 3.8%)	
Benign	14 (41.2%)	10 (100.0%)	4 (16.7%)	83.3% (68.4 to 98.2%)	
Malignant	11 (32.4%)	0 (0.0%)	11 (45.8%)	-45.8% (-65.8 to -25.9%)	
Highly malignant	8 (23.5%)	0 (0.0%)	8 (33.3%)	-33.3% (-52.2 to -14.5%)	
NSE !					

>33ug/L, n (%)	30 (71.4%)	5 (33.3%)	25 (92.6%)	-59.3% (-85.1 to -33.4%)	<0.001
Time to CT, min					
Mean (SD)	101 (80)	112 (73)	93 (84)	19 (-16 to 54)	0.29
Median [lq, uq]	80 [60,120]	90 [60,120]	73 [60,105]	0.61 (0.49 to 0.72)	0.08
Time between CT & death, days[a]					
Median [lq, uq]	2.0 [1.0,3.0]	N/A	2.0 [1.0,3.0]		
NECT - n (%)					0.001
No signs of hypoxia	66 (75.9%)	31 (93.9%)	35 (64.8%)	29.1% (14.0 to 44.2%)	
Equivocal	8 (9.2%)	2 (6.1%)	6 (11.1%)	-5.1% (-16.7 to 6.6%)	
Signs of hypoxia	13 (14.9%)	0 (0.0%)	13 (24.1%)	-24.1% (-35.5 to -12.7%)	
Number of patterns per patient -n (%)					
Mean (SD)	2.9 (1.8)	1.7 (1.4)	3.6 (1.7)	-1.9 (-2.6 to -1.2)	<0.001
Median [lq, uq]	3.0 [2.0,4.0]	2.0 [0.00,3.0]	3.5 [2.0,5.0]	0.21 (0.13 to 0.33)	<0.001
Number of patterns per patient – n (%)					<0.001

No patterns	10 (11.5%)	10 (30.3%)	0 (0.0%)	30.3% (14.6 to 46.0%)	
1 pattern	9 (10.3%)	3 (9.1%)	6 (11.1%)	-2.0% (-14.9 to 10.9%)	
2 patterns	20 (23.0%)	10 (30.3%)	10 (18.5%)	11.8% (-7.0 to 30.6%)	
3 patterns	17 (19.5%)	6 (18.2%)	11 (20.4%)	-2.2% (-19.2 to 14.8%)	
4 patterns	14 (16.1%)	4 (12.1%)	10 (18.5%)	-6.4% (-21.6 to 8.8%)	
5 patterns	11 (12.6%)	0 (0.0%)	11 (20.4%)	-20.4% (-31.1 to -9.6%)	
6 patterns	3 (3.4%)	0 (0.0%)	3 (5.6%)	-5.6% (-11.7 to 0.6%)	
7 patterns	2 (2.3%)	0 (0.0%)	2 (3.7%)	-3.7% (-8.7 to 1.3%)	
8 patterns	1 (1.1%)	0 (0.0%)	1 (1.9%)	-1.9% (-5.4 to 1.7%)	

Table 1: Summary of the study data including demography, durations, EEG, NSE results, NECT and number of perfusion patterns.

The median duration was recorded as zero minutes, indicating instances where it was less than a minute).

Abbreviations: EEG = Electroencephalogram, NSE = Neuron specific enolase,

, NECT = Nonenhanced CT, CI= confidence interval LQ= Lower quartile; SD = Standard deviation, UQ = Upper quartile.

*data available for only 80 patients,

[#] data available for only 86 patients

† data available for only 34 patients

[!] data available for only 42 patients

[a] data available for only 49 patients

Pattern				Sensitivity (95%-CI)	Specificity (95%-CI)	PPV (95%-CI)	NPV (95%-CI)	False Positive Rate (95%-CI)	Precision (95%-CI)	Accuracy (95%-CI)
Diffuse supra and infratentorial hypoperfusion	6	4	2	7.4% (2.1 to 17.9%)	93.9% (79.8 to 99.3%)	66.7% (22.3 to 95.7%)	38.3% (27.7 to 49.7%)	6.1% (0.7 to 20.2%)	6.1% (0.7 to 20.2%)	40.2% (29.7 to 50.7%)
Diffuse hypoperfusion of the supratentorial cortical grey matter	43	28	15	51.9% (37.8 to 65.7%)	54.5% (36.4 to 71.9%)	65.1% (49.1 to 79.0%)	40.9% (26.3 to 56.8%)	45.5% (28.1 to 63.6%)	45.5% (28.1 to 63.6%)	52.9% (42.2 to 63.6%)
Regional cortical hypoperfusion	7	6	1	11.1% (4.2 to 22.6%)	97.0% (84.2 to 99.9%)	85.7% (42.1 to 99.6%)	40.0% (29.2 to 51.6%)	3.0% (0.1 to 15.8%)	3.0% (0.1 to 15.8%)	43.7% (33.0 to 54.3%)
Hypoperfusion of the basal ganglia	33	27	6	50.0% (36.1 to 63.9%)	81.8% (64.5 to 93.0%)	81.8% (64.5 to 93.0%)	50.0% (36.1 to 63.9%)	18.2% (7.0 to 35.5%)	18.2% (7.0 to 35.5%)	62.1% (51.7 to 72.5%)
Hypoperfusion of the thalamus	20	18	2	33.3% (21.1 to 47.5%)	93.9% (79.8 to 99.3%)	90.0% (68.3 to 98.8%)	46.3% (34.0 to 58.9%)	6.1% (0.7 to 20.2%)	6.1% (0.7 to 20.2%)	56.3% (45.7 to 67.0%)
Hypoperfusion of the brainstem	13	13	0	24.1% (13.5 to 37.6%)	100.0% (89.4 to 100.0%)	100.0% (75.3 to 100.0%)	44.6% (33.0 to 56.6%)	0.0% (0.0 to 10.6%)	0.0% (0.0 to 10.6%)	52.9% (42.2 to 63.6%)
Diffuse perfusion delay	31	19	12	35.2% (22.7 to 49.4%)	63.6% (45.1 to 79.6%)	61.3% (42.2 to 78.2%)	37.5% (24.9 to 51.5%)	36.4% (20.4 to 54.9%)	36.4% (20.4 to 54.9%)	46.0% (35.3 to 56.7%)

Regional perfusion delay	15	12	3	22.2% (12.0 to 35.6%)	90.9% (75.7 to 98.1%)	80.0% (51.9 to 95.7%)	41.7% (30.2 to 53.9%)	9.1% (1.9 to 24.3%)	9.1% (1.9 to 24.3%)	48.3% (37.6 to 59.0%)
Hypoperfusion of the white matter	5	3	2	5.6% (1.2 to 15.4%)	93.9% (79.8 to 99.3%)	60.0% (14.7 to 94.7%)	37.8% (27.3 to 49.2%)	6.1% (0.7 to 20.2%)	6.1% (0.7 to 20.2%)	39.1% (28.6 to 49.5%)
Bilateral borderzone perfusion delay	13	10	3	18.5% (9.3 to 31.4%)	90.9% (75.7 to 98.1%)	76.9% (46.2 to 95.0%)	40.5% (29.3 to 52.6%)	9.1% (1.9 to 24.3%)	9.1% (1.9 to 24.3%)	46.0% (35.3 to 56.7%)
Territorial infarctions(s)	5	3	2	5.6% (1.2 to 15.4%)	93.9% (79.8 to 99.3%)	60.0% (14.7 to 94.7%)	37.8% (27.3 to 49.2%)	6.1% (0.7 to 20.2%)	6.1% (0.7 to 20.2%)	39.1% (28.6 to 49.5%)
Reduction in the gradient between gray and white matter in CBV	33	28	5	51.9% (37.8 to 65.7%)	84.8% (68.1 to 94.9%)	84.8% (68.1 to 94.9%)	51.9% (37.8 to 65.7%)	15.2% (5.1 to 31.9%)	15.2% (5.1 to 31.9%)	64.4% (54.1 to 74.6%)
Supratentorial hypoperfusion with infratentorial hyperperfusion	15	11	4	20.4% (10.6 to 33.5%)	87.9% (71.8 to 96.6%)	73.3% (44.9 to 92.2%)	40.3% (28.9 to 52.5%)	12.1% (3.4 to 28.2%)	12.1% (3.4 to 28.2%)	46.0% (35.3 to 56.7%)
Hyperperfusion	4	4	0	7.4% (2.1 to 17.9%)	100.0% (89.4 to 100.0%)	100.0% (39.8 to 100.0%)	39.8% (29.2 to 51.1%)	0.0% (0.0 to 10.6%)	0.0% (0.0 to 10.6%)	42.5% (31.9 to 53.1%)

Table 2: Summary of the diagnostic performance of the most frequent perfusion patterns in predicting unfavourable outcome or death.

Abbreviations: CBV = Cerebral blood flow, CI = Confidence interval.

Low frequency of the following patterns, therefore, not reported: Regional cortical hypoperfusion sparing the motor cortex, Hypoperfusion of the globus pallidus, cerebellar hypoperfusion, asymmetric hypoperfusion

Author contribution:

Arsany Hakim: Conceptualisation, methodology, formal analysis, data curation, visualisation, Writing– original draft

Mattia Branca: Formal analysis, writing– review and editing

Christoph Kurmann: Data curation, writing– review and editing

Benedikt Wagner: Data curation, writing– review and editing

Manuela Iten: Resources, data curation, writing– review and editing

Matthias Hänggi: Conceptualisation, resources, data curation, writing– review and editing

Franca Wagner: Validation, writing– review and editing

Declaration of interest: none

Declaration of interests

☒ The authors declare that they have no known competing financial interests or personal relationships that could have appeared to influence the work reported in this paper.

☐ The authors declare the following financial interests/personal relationships which may be considered as potential competing interests: